Average Structure of Rb_2ZnBr_4

By C. J. de Pater

Werkgroep Fysische Kristallografie, Afdeling Technische Natuurkunde, Technical University Delft, Lorentzweg 1, Delft, The Netherlands

Abstract

The average structure of Rb_2ZnBr_4 has been determined from neutron diffraction powder diagrams at 373, 300 and 4·2 K. These temperatures correspond to the three known phases: the normal high-temperature phase, the incommensurate phase (between 355 and 200 K) and the phase with a tripled c axis. The basic lattice space group is found to be *Pcmn* and the structure is of the β-K_2SO_4 type. In the average structure refinement, in the low-temperature phases, the displacement wave is observed as anisotropic smearing-out of the atoms. It is found that the average anisotropic component of the amplitude is independent of temperature, which means that the long-range correlated atomic displacements in the incommensurate phase go over into uncorrelated displacements in the high-temperature phase.

(I) Introduction

The room-temperature diffraction pattern of Rb_2ZnBr_4 shows satellite reflections which are typical for a modulated structure. Related materials with a modulated phase are K_2SeO_4 (Iizumi, Axe, Shirane & Shimaoka, 1977) and $(NH_4)_2BeF_4$ (Iizumi & Gesi, 1977). The latter compounds were found to possess the β-K_2SO_4 structure. From the cell constants it was concluded that Rb_2ZnBr_4 also has the β-K_2SO_4 structure (Struikmans, 1978). The average-structure space group is presumably *Pcmn* or $Pc2_1n$ (where the pseudo-hexagonal axis is denoted as the c axis), as determined from systematic extinctions in the diffraction pattern.

Rb_2ZnBr_4 has orthorhombic symmetry from the melting point down to helium temperature. However, below 355 K the lattice is deformed by an incommensurate displacement wave (de Pater & van Dijk, 1978) which is characterized by a wave vector $q_0 = 0·292c^*$. At about 200 K the wave vector locks in to $\frac{1}{3}c^*$ and the crystal becomes ferroelectric with spontaneous polarization in the b direction.

Of course, a structure determination is essential for an understanding of the phase transitions. The preliminary structure refinements presented here were undertaken on the basis of neutron diffraction powder

diagrams since the low incoherent cross-section in the case of neutron diffraction favours this method rather than X-ray diffraction. An X-ray single-crystal determination of the structure at room temperature has been undertaken and is in process (de Jager, 1978).

(II) Experimental

The neutron powder diagrams were obtained on a diffractometer at ECN (Petten), with $\lambda = 2·57$ Å. The structure was refined with the profile method (Rietveld, 1969). Horizontal collimation was 30' (both in front of the monochromator and the counter) for the 4·2 K and the 373 K diagrams; for the 300 K diagram 10' collimation slits were used. For the purpose of comparing the crystal structure at several temperatures it is sufficient to collect data with 30' collimation slits; tight collimation was employed at 300 K in order to obtain the best possible result at that temperature. In the instrumental range of 140° in 2θ, 220 reflections are found, resulting in severe overlap of the peaks. All satellite reflections are relatively weak compared to the strong main reflections (Struikmans, 1978) (*i.e.* less than 5%). Separately observed satellites were excluded from the calculation, since only the average structure was refined corresponding to main reflections in the diffraction pattern. It is impossible to carry out a complete refinement of the structure on the basis of powder data, in view of the overlap of the weak satellite reflections with main reflections.

(III) Results

First, the structure was refined at 300 K in space group *Pcmn*. Since no satellite reflections are found in the a^*c^* plane the displacement wave is b-polarized. That is to say, atoms in the mirror plane shift along b; the tetrahedral $ZnBr_4$ groups are allowed to rotate about the a and c axes. Since only main reflections were used in the refinement the displacement wave is observed by an anisotropic smearing-out of the atoms. This is simulated in the structure refinement by splitting them up in accordance with the polarization of the wave. An overall isotropic Debye–Waller factor was applied;

individual Debye–Waller factors did not significantly improve the fit. The resulting fit to the measured profile was good, as shown in Fig. 1.

The significance of the splitting of the atoms was tested by refining the structure without split atoms. The R factor on the basis of intensities* (Rietveld, 1969) was twice as high for the latter model as compared to the former. Consequently, the splitting is significant although the split-atom model requires eight parameters more than the model without split atoms.

In Fig. 2 the structure is drawn in two projections. It is seen that appreciable rotations of the $ZnBr_4$ groups about the pseudo-triad axis occur, as well as rotations about the a axis. The atomic positions are listed in Table 1. The corresponding bond lengths and angles of the $ZnBr_4$ tetrahedron are listed in Table 2, together with the average nearest-neighbour distances of the two Rb sites. The tetrahedron is far from regular as is usually found in Zn–halogenide groups (Gibbons, Reinsborough & Whitla, 1975; Morosin & Lingafelter, 1959). Probably, the Zn–Br bonds are not very much stronger than the Br–Rb bonds. The lengths of the latter depart strongly from each other for the three Br sites, which in fact may explain the deformation of the tetrahedron. The strength of the Zn–Br bonds can be derived from the frequency of the breathing mode of the $ZnBr_4$ group, whereas the strength of the Rb–Br bonds is related to the Debye cut-off frequency. The frequency of the breathing mode $(17 \cdot 2 \text{ mm}^{-1})$ is only 30% higher than the estimated Debye cut-off frequency in Rb_2ZnBr_4 (de Pater & van Dijk, 1978). The frequency of the breathing mode is taken from Quicksall & Spiro

(1966). The helium temperature diagram was analysed in a similar way with split atoms, and using space group $Pcmn$. The real space group at this temperature is $Pc2_1n$, with a tripled c axis (de Pater, 1978). However, the deviation from the inversion symmetry of the average structure is supposed to be small. Anyway, the polar space group yielded no significant decrease of the R factor. Consequently the deviation of the average structure from inversion symmetry, as obtained in a refinement using space group $Pc2_1n$ is not significant, justifying the use of space group $Pcmn$.

Above the incommensurate transition temperature a structure refinement was also carried out. The vanishing of the satellite reflections might be supposed to correspond to a disappearance of the splitting. However, at 373 K a significant smearing-out was still observed. In the analysis of the 373 K diagram, split atoms were used to simulate anisotropic smearing-out of the atoms in the structure model, since the computer program has the possibility of assigning only an isotropic Debye–Waller factor to each atom.

In this case we assigned individual isotropic Debye–Waller factors to the atoms. Just as for the room-temperature structure refinement we tested the significance of the split-atom model for both the 4·2 K and the 373 K structure refinements. Approximately the same R factor ratios were obtained, from which the conclusion can be drawn that at all three temperatures there is a significant anisotropic smearing-out of the atoms.

---

* See Rietveld (1969) for a derivation of the R factor, in the case of the profile method.
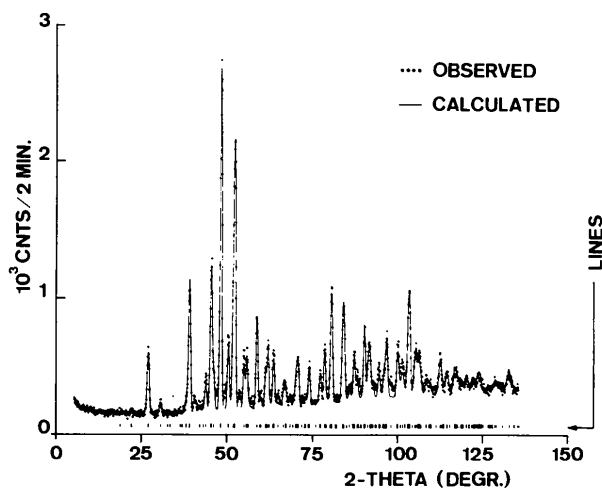

Fig. 1. Neutron diffraction powder diagram at 300 K. The calculated diagram is fitted to the raw data minus a graphically determined background.
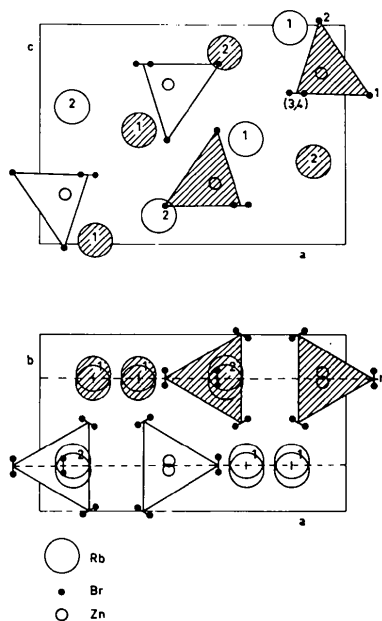

Fig. 2. Structure of Rb_2ZnBr_4 at 300 K projected on ac and ab. In the ab projection some of the atoms which coincide with the Zn atom are omitted.

Table 1. *Fractional coordinates of* Rb_2ZnBr_4 *at three temperatures*

Standard deviations are indicated in parentheses. The Debye–Waller factors are listed in Table 3. For a definition of the R factor and residual, see Rietveld (1969).

	T = 4·2 K			T = 300 K			T = 373 K			
	x	y	z	x	y	z	x	y	z	B(Å²)
Rb(1)	0·179 (1)	0·281 (5)	0·017 (2)	0·175 (1)	0·268 (5)	0·017 (1)	0·173 (1)	0·272 (11)	0·010 (2)	4·5 (10)
Rb(2)	0·903 (1)	0·288 (5)	0·372 (2)	0·900 (1)	0·287 (3)	0·373 (1)	0·897 (1)	0·275 (11)	0·373 (2)	6·6 (10)
Zn	0·924 (2)	0·237 (11)	0·781 (2)	0·923 (1)	0·224 (4)	0·774 (1)	0·925 (2)	0·291 (6)	0·766 (2)	3·3 (10)
Br(1)	0·925 (2)	0·294 (3)	0·022 (1)	0·920 (1)	0·289 (2)	0·019 (1)	0·920 (2)	0·275 (10)	0·017 (2)	7·4 (8)
Br(2)	0·086 (2)	0·301 (4)	0·662 (2)	0·088 (2)	0·289 (2)	0·678 (2)	0·090 (1)	0·300 (3)	0·680 (2)	1·5 (7)
Br(3)	0·803 (2)	0·483 (5)	0·703 (3)	0·819 (1)	0·477 (3)	0·685 (3)	0·827 (3)	0·472 (5)	0·672 (3)	3·5 (6)
Br(4)	0·863 (2)	0·524 (5)	0·680 (3)	0·863 (1)	0·524 (3)	0·683 (3)	0·862 (2)	0·530 (5)	0·696 (3)	3·5 (6)

Lattice parameters (Å)			
a	13·140 (3)	13·330 (3)	13·386 (3)
b	7·595 (2)	7·656 (2)	7·679 (2)
c	9·601 (2)	9·707 (2)	9·753 (2)

R (profile)	18%	18%	17%
Residual	17	4	7

Table 2. *Interatomic distances* (Å) *and angles* (°) *of* Rb_2ZnBr_4 *at* 300 K

(a) Within the $ZnBr_4$ group, between average atomic positions

Zn–Br(1)	2·39 (2)	Br(1)–Zn–Br(2)	114
Zn–Br(2)	2·39 (2)	Br(1)–Zn–Br(3,4)	111
Zn–Br(3,4)	2·37 (2)	Br(2)–Zn–Br(3,4)	106
Br(1)–Br(2)	4·00 (2)	Br(3,4)–Zn–Br(3,4)	108
Br(1)–Br(3,4)	3·92 (2)		
Br(2)–Br(3,4)	3·81 (3)		
Br(3,4)–Br(3,4)	3·83 (3)		

(b) Average Rb–Br$_n$ distances (where $n = 9$ or 10)

Rb(1)–Br$_9$	3·61
Rb(2)–Br$_{10}$	3·86

Table 3 lists the splitting amplitudes at three temperatures, as well as the overall Debye–Waller factors and the average Debye–Waller factor at 373 K.

(IV) Discussion

On comparing the results at different temperatures we note two features. The Debye–Waller factor seems to be a good measure of the thermal amplitude since it is nearly zero at helium temperature. At room temperature the Debye–Waller factor is already high indicating large thermal vibrations. This is in agreement with the softness of the material (de Pater & van Dijk, 1978).

Secondly, the splitting of the atoms is nearly equal at all temperatures. This seems puzzling since the satellite intensities were found to decrease by a factor of 100 between the helium temperature and the incommensurate-to-normal transition, where the diffuse intensity is measured at the latter temperature, as given by de Pater & van Dijk (1978). From the structure refinements one may derive the following mechanism of the transition. In the normal phase, large but uncorrelated atomic displacements occur which can be separated into an isotropic and an anisotropic component. Upon lowering the temperature the overall isotropic thermal amplitude decreases, while the anisotropic component remains constant. In Fig. 3 the temperature dependence of both components is plotted. The transition occurs at a temperature where the two components are in approximately equal proportions. In the low-

Table 3. *Splitting amplitudes at the three temperatures* (Å) $\overline{(u^2)}^{1/2} = (B/4\pi^2)^{1/2}$

	T = 4·2 K			T = 300 K			T = 373 K		
	Δx	Δy	Δz	Δx	Δy	Δz	Δx	Δy	Δz
Rb(1)		0·24 (4)			0·14 (4)			0·17 (8)	
Rb(2)		0·29 (4)			0·28 (2)			0·19 (8)	
Zn		0·10 (8)			0·20 (3)			0·31 (5)	
Br(1)		0·33 (2)			0·30 (2)			0·19 (8)	
Br(2)		0·39 (3)			0·29 (2)			0·38 (2)	
Br(3,4)	0·20 (3)	0·08 (4)	0·06 (3)	0·15 (1)	0·09 (2)	0·01 (3)	0·23 (3)	0·22 (4)	0·12 (6)

B (Å²)	0·21 (18)	2·6 (1)	4·3 (7)
$\overline{(u^2)}^{1/2}$ (Å)	0·07 (6)	0·26 (1)	0·33 (5)

temperature phase the static long-range ordered displacement wave (corresponding to the satellite reflections) takes the place of the thermal displacements in the high-temperature phase. The present results agree with the findings of inelastic neutron-scattering studies (de Pater & van Dijk, 1978; de Pater, Axe & Currat, 1978). In these measurements a rather strong quasi-elastic diffuse peak was observed at high temperature (423 K) which is centred in reciprocal space at a wave vector of $0.29c^*$. This diffuse scattering is due to short-range correlated displacement fluctuations and an energy analysis yielded a relaxation time for the fluctuations of 2×10^{-11} s, at 423 K.
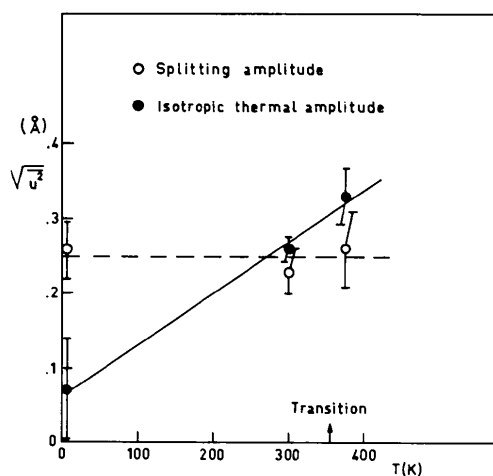
In the present structure refinement these fluctuations in the normal high-temperature phase are seen as anisotropic smearing-out of the atoms.

In the low-temperature phase satellite reflections appear and the diffuse-scattering intensity decreases. The static displacements are seen as the splitting up of the atoms in the average structure. The splitting amplitude remains nearly constant in view of the decrease of the anisotropic thermal amplitude.

Fig. 3. Temperature dependence of the isotropic thermal amplitude: $(\overline{u^2})^{1/2} \equiv (B/4\pi^2)^{1/2}$, where B is the overall Debye–Waller factor. The average splitting amplitude is also plotted, calculated from the data in Table 3.

References

GIBBONS, C. S., REINSBOROUGH, V. C. & WHITLA, W. A. (1975). Can. J. Chem. 53, 114–118.

IIZUMI, M., AXE, J. D., SHIRANE, G. & SHIMAOKA, K. (1977). Phys. Rev. B, 15, 4392–4411.

IIZUMI, M. & GESI, K. (1977). Solid State Commun. 22, 37–42.

JAGER, G. DE (1978). Private communication.

MOROSIN, B. & LINGAFELTER, E. C. (1959). Acta Cryst. 12, 744–745.

PATER, C. J. DE (1978). Phys. Status Solidi A, 48, 503–512.

PATER, C. J. DE, AXE, J. D. & CURRAT, R. (1978) Unpublished.

PATER, C. J. DE & VAN DIJK, C. (1978). Phys. Rev. B, 18, 1281–1283.

QUICKSALL, C. O. & SPIRO, T. G. (1966). Inorg. Chem. 5, 2232–2233.

RIETVELD, H. M. (1969). J. Appl. Cryst. 2, 65–71.

STRUIKMANS, R. (1978). Private communication.

The Crystal Structure of Ag_2INO_3

BY KENNETH PERSSON

Physical Chemistry 1, Chemical Center, University of Lund, POB 740, S-220 07 Lund 7, Sweden

Abstract

Ag_2INO_3 is orthorhombic, space group $P2_12_12_1$ with $a = 7.4354$ (4), $b = 7.7759$ (4), $c = 17.1338$ (12) Å, and $Z = 8$. The structure was solved by direct methods from diffractometer data and was refined aniso-tropically to an R value of 0.029. The I atoms are coordinated to six Ag atoms forming trigonal prisms which build up chains by sharing edges. The chains are linked together by either corners or edges. The NO_3 groups are located in the cavities of this three-dimensional network.